HHS Public Access

Author manuscript

*Biochemistry*. Author manuscript; available in PMC 2020 February 13.

Published in final edited form as:

*Biochemistry*. 2020 February 11; 59(5): 682–693. doi:10.1021/acs.biochem.9b00896.

# Length specificity and polymerization mechanism of (1,3)-β-D-glucan synthase in fungal cell wall biosynthesis

**Abhishek Chhetri**[1,#], **Anna Loksztejn**[1,#], **Hai Nguyen**[1], **Kaila M. Pianalto**[2], **Mi Jung Kim**[3], **Jiyong Hong**[3], **J. Andrew Alspaugh**[2], **Kenichi Yokoyama**[1,3,*]

[1]Department of Biochemistry, Duke University School of Medicine

[2]Department of Medicine, Duke University School of Medicine

[3]Department of Chemistry, Duke University

## Abstract

(1,3)-β-D-Glucan synthase (GS) catalyzes formation of the linear (1,3)-β-D-glucan in the fungal cell wall, and is a target of clinically approved antifungal antibiotics. The catalytic subunit of GS, FKS protein, does not exhibit significant sequence homologies to other glycosyltransferases, and thus a significant ambiguity remains about its catalytic mechanism. One of the major technical barriers in studying GS is the absence of activity assay methods that allow characterization of the lengths and amounts of (1,3)-β-D-glucan due to its poor solubility in water and organic solvents. Here, we report a successful development of a novel GS activity assay based on size-exclusion chromatography coupled with pulsed-amperometric detection and radiation counting (SEC-PAD-RC), which allows for the simultaneous characterization of the amount and length of the polymer product. The assay revealed that the purified yeast GS produces glucan with a length of 6,550 ± 760 mer, consistent with the reported degree of polymerization of (1,3)-β-D-glucan isolated from intact cells. Pre-steady state kinetics analysis revealed a highly efficient but rate-determining chain elongation rate of 51.5 ± 9.8 $sec^{-1}$, which represents the first observation of chain elongation by a nucleotide-sugar dependent polysaccharide synthase. Coupling the SEC-PAD-RC method with substrate analog mechanistic probes provided the first unambiguous evidence that GS catalyzes non-reducing end polymerization. Based on these observations, we propose a detailed

[*]**Corresponding Author:** Please address all correspondence to: ken.yoko@duke.edu.
[#]These authors contributed equally.



ASSOCIATED CONTENT

The materials and methods used in this study are described in detail in SI Appendix. Information includes procedures for preparation of *Saccharomyces cerevisiae fks2Δ*, minimum inhibitory concentration assays, GS preparation, GS assays by quantitation of glucan, UDP and Glc, GS assays using HPAEC and SEC-PAD-RC, $IC_{50}$ determination of GS-targeting antifungals and UDP-Glc analogs, preparation and characterization of UDP-Glc analogs, and MS characterization of GS. The Supporting Information is available free of charge on the ACS Publications website. Accession codes: FKS1 (UniProt ID P38631), and Rho1 (UniProt ID P06780).

model for the catalytic mechanism of GS. The approaches described here can be used to determine the mechanism of catalysis of other polysaccharide synthases.

**Keywords**

(1,3)-β-D-glucan synthase; fungal cell wall; polysaccharide biosynthesis; antifungal; glycosyltransferase

## Introduction

Invasive fungal infections are becoming more common due to increasing numbers of immunocompromised patients and travelers through endemic regions [1]. Current treatment options are constrained by limited activity spectra, increasing drug resistance, and the high toxicity of existing antifungals [2]. The major challenge in antifungal development is the difficulty in selectively killing fungi without severe toxicity to humans. For this reason, essential enzymes involved in fungal cell wall biosynthesis represent attractive antifungal targets as these enzymes are absent in humans.

The fungal cell wall consists of two layers. The outer layer is composed of mannoproteins, and the inner layer is a mixture of glucan and chitin and maintains the physical strength of the cell wall [3, 4]. Of the inner cell wall constituents, (1,3)-β-D-glucan is frequently the major polysaccharide component [4]. (1,3)-β-D-glucan is first biosynthesized by (1,3)-β-D-glucan synthase (GS) and deposited into the periplasmic space (Fig. 1A). Subsequently, the (1,3)-β-D-glucan is elongated, branched, and crosslinked to other constituents [3]. Due to the critical role of GS in fungal cell wall formation and fungal physiology, GS is targeted by three structurally distinct classes of naturally occurring antifungal agents (Fig. 1B) [5].

GS is composed of a catalytic subunit, Fks1p, Fks2p or Fks3p in *S. cerevisiae*, and a regulatory subunit, Rho1p. The stoichiometry of the two subunits and their oligomeric states are not known. The catalytic subunit catalyzes the homopolymerization of D-glucose (Glc) using UDP-Glc as its substrate (Fig. 1A) [5, 6]. GS is catalytically active when the Rho1p GTPase is bound to GTP and inactive when it is bound to GDP. Fks1p is responsible for the formation of bulk (1,3)-β-D-glucan in the cell wall during vegetative growth, and responsible for the in vitro activity of GS [7]. Fks2p, regulated by calcineurin and the cell integrity signaling pathway, is responsible for cell wall formation during stress conditions, such as high temperature or limited glucose availability [8]. Fks3p is responsible for the formation of (1,3)-β-D-glucan in the spore cell wall, and does not contribute to the in vitro activity of GS [7].

Intriguingly, the catalytic subunit, FKS, does not exhibit significant sequence homologies to other functionally characterized glycosyltransferases, and has been classified to form a unique family of GT48. This unique amino acid sequence of FKS made it impossible to compare the catalytic function and mechanism of FKS to other glycosyltransferases. As a result, significant ambiguity remains about even the most fundamental aspects of GS catalysis, such as the length of polymer products and the direction of polymerization.

In particular, the length of (1,3)-β-D-glucan produced by GS is important to understand the mechanism by which (1,3)-β-D-glucan is biosynthesized and integrated into the cell wall. Based on existing literature, two mechanisms are conceivable (Fig. 1A). In the first mechanism, GS catalyzes the formation of 60–80 mer (1,3)-β-D-glucan that is subsequently modified in the periplasm through mainchain elongation, branching and side chain elongation (Fig. 1A, path A). This model is based on an early report that crude *S. cerevisiae* GS produces (1,3)-β-D-glucan with an average length of 60–80 mer [6], which is significantly shorter than the widely reported degree of polymerization (DP) of (1,3)-β-D-glucan in the cell wall (~1,500 – 8,000) [9, 10]. The elongation of the short polysaccharides into full length glucan has been proposed to be catalyzed by (1,3)-β-D-glucanosyltransferases [11–13]. These enzymes catalyze an endo-type splitting of a (1,3)-β-D-glucan, followed by ligation of the newly generated reducing end to the non-reducing end of another (1,3)-β-D-glucan molecule causing elongation or branching [11, 14]. Supporting this model, Gas1p knockout in *S. cerevisiae* resulted in (1,3)-β-D-glucan with lower molecular weights, although the actual length was not determined [13, 15, 16]. Similarly, Gel4p, a Gas1p homolog in *Aspergillus fumigatus*, was proposed to catalyze (1,3)-β-D-glucan elongation based on its *in vitro* activity to catalyze elongation of short (1,3)-β-D-glucan and was essential for the viability of the organism [12].

In the second possible mechanism of (1,3)-β-D-glucan incorporation into the fungal cell wall, GS directly catalyzes the formation of large linear (1,3)-β-D-glucan (DP of ~1,500 – 8,000) that is then modified by (1,3)-β-D-glucanosyltransferases, introducing branching and side-chain-elongation (Fig. 1A, path B). Gas1p was recently shown to be responsible for (1,6)-β-branch formation both in vitro and in vivo [11]. In this model, the length of GS products defines the DP of (1,3)-β-D-glucan in the cell wall because the subsequent branching and side chain elongation proceeds through a rearrangement of linear (1,3)-β-D-glucan without affecting the overall DP. Therefore, understanding the length of GS-produced (1,3)-β-D-glucan is critical to understand the mechanism of early steps of the fungal cell wall biosynthesis.

Another unanswered question in the GS catalytic mechanism is the direction of polymerization. Nucleotide-sugar dependent polysaccharide biosynthesis can proceed either at the reducing end or non-reducing end (Fig. 2). The two mechanisms are difficult to distinguish and have been characterized for only a few enzymes. In those previous studies, the direction of polymerization has been studied by characterizing short oligomeric intermediates or priming substrates, or by pulse-chase experiments with radioactive substrates. Non-reducing end polymerization was proposed for chitin synthase based on the characterization of short chitooligomers produced in *in vitro* assays using GlcNAc, short chitooligomers, and their derivatives as priming substrates [17]. Hyaluronan synthase was proposed to catalyze reducing end polymerization based on pulse-chase experiments as well as characterization of short oligosaccharide intermediates [18, 19]. For plant starch synthase, results from pulse-chase experiments were initially interpreted to support reducing end polymerization [20], while recent characterization of short oligomers produced by recombinant enzymes suggested the non-reducing end polymerization model [21]. Unfortunately, these approaches are unsuitable to characterize GS as GS does not accumulate short oligomeric intermediates, no priming substrates have been identified, and

the length specificity and kinetics of polymerization critical to design the pulse-chase experiments are unknown. These technical challenges are likely the case for many other polysaccharide synthases, and a generally applicable approach to study their mechanisms is needed.

The studies on GS catalytic mechanisms have been hampered by the technical challenges associated with the quantitative characterization of (1,3)-β-D-glucan that is insoluble in water and most organic solvents commonly used for chromatographic analysis. In this report, we describe the development of a size exclusion chromatography (SEC) based method and a set of mechanistic probes to characterize GS function and mechanism in detail. The assay exploits the unique solubility of (1,3)-β-D-glucan in strong basic solutions, allowing characterization using SEC coupled with pulsed amperometric detection (PAD) and radiation counting (RC). These developments allowed the determination of the length and the amount of (1,3)-β-D-glucan with pmol sensitivity. Application of this method revealed that purified GS produces (1,3)-β-D-glucan with the degree of polymerization (DP) of 6,550 ± 760, which is much longer than previous report (DP 60–80) and comparable to the DP of (1,3)-β-D-glucan in yeast cell walls. The assay also allowed detailed mechanistic characterization. Time-course analysis revealed a pre-steady state phase in which the glucan chain is elongated processively with a rate of ~50 $sec^{-1}$, providing the first kinetic insights into the GS catalysis. The observed rate of elongation by GS is > 100-folds faster than those reported for β-glucanosyltransferase, suggesting that GS is likely the predominant factor determining the overall DP of (1,3)-β-D-glucan in the cell wall. As the rapid kinetics precluded the ability to use pulse-chase experiments to characterize the direction of elongation, we utilized 1’- and 3’-blocked substrate analogs with our SEC-PAD-RC method to determine that GS catalyzes polymer formation by non-reducing end polymerization. Based on our observations, we propose a refined function of GS in the fungal cell wall biosynthesis and a catalytic cycle model for GS catalysis consisting of initiation, elongation, and termination. The combination of blocked substrate analogs and the product length characterization described here is applicable to other polysaccharide synthases and could improve our general understanding of polysaccharide biosynthetic mechanisms.

## Materials and Methods

### General.

CHAPS was purchased from VWR. Cholesteryl hemisuccinate was purchased from Anatrace. UDP-Glc and GTPγS were purchased from Millipore Sigma. UDP-[$^{14}$C]Glc was purchased from American Radiolabeled Chemicals. Casponfungin was purchased from Merck or Millipore Sigma, and micafungin from Astellas. Other common chemicals were purchased from VWR or Millipore Sigma with ACS grade or equivalent. Nonlinear least-squares fitting of kinetic and inhibition data was carried out using the MATLAB curve fitting toolbox (The MathWorks, Inc., Natick, MA). HPLC experiments were performed on a Dionex ICS 5000+ instrument equipped with diode array (Dionex PDA) and electrochemical detectors (Dionex ICS-5000+ DC) and an autosampler (Dionex AS-AP). Electrochemical detection was performed using standard carbohydrate disposable electrodes (Thermo Fisher Scientific) with the Gold, Carbo, Quad waveform. HPAEC was performed using either a

CarboPac PA200 or DNAPac PA100 BioLC column (Thermo Fisher Scientific) and size exclusion chromatography (SEC) was performed using an Acclaim SEC-1000 column (Thermo Fisher Scientific), all at 30 °C. Protein concentrations were determined using either the Pierce 660nm Protein Assay (Thermo Fisher Scientific) or EZQ Protein Quantitation Kit (Invitrogen) using bovine serum albumin as a protein standard. Radioactivity counting (RC) was performed using Hydrofluor (National Diagnostics) counting solution and a Beckman LS 6500 scintillation counter. UV-vis spectra were determined using a Hitachi U-3900H or a FLUOStar Optima plate reader (BMG Labtech). *S. cerevisiae* strains used in this study are summarized in Table S3. Enfumafungin was provided by Dr. Gerald Bills at University of Texas Health Science Center at Houston. Anti-Gas1p antibody was provided by Dr. Yoichi Noda at the University of Tokyo and Dr. Randy Shekman at University of California, Berkeley. Anti-Rho1p antibody was provided by Dr. Yoshikazu Ohya. Anti-FKS antibody was provided by Dr. Jean-Paul Latgé at the Institut Pasteur.

## Preparation of Saccharomyces cerevisiae fks2Δ.

To create the *FKS2* deletion strain in the BY4741 (S288c) background [22], the entire *S. cerevisiae FKS2* (YGR032W) open reading frame was replaced with the natMX4 marker [23]. The deletion construct consisted of 40 bp of flanking sequence 5' to the *FKS2* open reading frame, the natMX4 marker amplified from pAG25, and 40 bp of flanking sequence 3' to the *FKS2* open reading frame. The construct was amplified using the PCR primers in Table S4. The deletion construct was introduced into *S. cerevisiae* using a modified lithium acetate/ssDNA carrier/polyethylene glycol (PEG) transformation protocol [24]. In brief, *S. cerevisiae* was grown to mid-log phase, then co-incubated with the deletion construct DNA in 33% PEG 3350, 0.1 M lithium acetate, and 0.2 mg/mL single-stranded salmon sperm DNA at 30°C for 30 minutes, then 42°C for 15 minutes. Transformed cells were recovered in YPD medium (yeast extract 20 g/L, peptone 10 g/L, and dextrose 2 g/L) at 30°C for 4 hours prior to plating on selective medium (YPD + 200 ug/mL nourseothricin).

## Preparation of GS.

*S. cerevisiae fks2Δ*, *S. cerevisiae gas1Δ* or *S. cerevisiae* BY4741 was grown in YPD media at 30 °C overnight, and 6 x 30 mL aliquots were used to inoculate 6 x 1.5 L of YPD media in 2.8 L baffled flasks. Cultures were grown at 30 °C until early log phase ($OD_{600}$ = 0.8–1.2), and harvested by centrifugation at 4 °C at 5,000 x *g* for 25 min. The pellets were washed with 10 mM EDTA pH 8.0, then stored at −80 °C. Typically, 50 g of the cell pellet was resuspended in 150 mL of ice-cold breaking buffer (0.5 M NaCl, 10 mM EDTA pH 8.0, 1 mM PMSF). The resuspended *S. cerevisiae* was disrupted using a bead beater (BioSpec) and 0.5 mm glass beads with 5 x 1 min pulses with 10 min of chilling on ice between each pulse. The lysate was clarified by centrifugation at 1,500 x g for 15 min at 4°C. The insoluble pellet was resuspended in 100 mL of the breaking buffer and disrupted on the bead beater as described above to give 90–95% lysis of *S. cerevisiae* as determined by phase contrast microscopy. The lysate was clarified by centrifugation as described above. The clarified supernatants from the two lysis steps were combined and ultra-centrifuged at 100,000 g for 1h at 4°C. The membrane pellets obtained were gently resuspended in 80 mL of membrane buffer (50 mM Tris pH 7.5, 10 mM EDTA, 1mM β-mercaptoethanol, 33% v/v glycerol) using a dounce homogenizer to give a solution of approximately 5 mg/mL protein

concentration. This suspension (membrane fraction) was flash-frozen and stored at −80 °C with minimal loss of activity. To solubilize GS in the membrane fraction, the frozen membrane fractions were thawed on ice, and the final concentrations of 27.5 μM GTPγS, 6.88 mM DTT, 192 mM NaCl, 0.688% CHAPS, and 0.138% CHS were added to the final volume of 112 mL. This suspension was homogenized, stirred for 30 min on ice, and ultra-centrifuged at 100,000 g for 30 min at 4°C. To begin product entrapment, the detergent soluble fraction was incubated with the final concentrations of 33 mM KF and 5 mM UDPGlc at 30 °C for 20–30 min and chilled on ice for 15 min. The insoluble (1,3)-β-d-glucan containing GS was collected by centrifugation at 5,000 g for 5 min at 4°C. The resulting colorless pellet was washed with five cycles of resuspension in 0.5 mL wash buffer (membrane buffer with 5 mM UDPGlc, 1mM DTT, 4 μM GTPγS, 0.4% CHAPS, 0.08% CHS), brief homogenization, and centrifugation at 5,000 x g at 4 °C. At the end of the fifth wash cycle, the pellet was collected by ultracentrifugation at 400,000 x g and 4°C for 10 min. To release GS from insoluble (1,3)-β-d-glucan, the resulting glucan pellet was resuspended and homogenized in 0.5 mL extraction buffer (membrane buffer with 1mM DTT, 4 μM GTPγS, 0.4% CHAPS, 0.08% CHS) and incubated overnight at 4 °C. The GS extraction was performed four more times with each cycle of extraction consisting of resuspention of the glucan pellet in 0.5 mL extraction buffer, homogenization, incubation on ice for 10 min, and centrifugation for 10 min at 400,000 x g. The supernatants were pooled to yield the product entrapment-purified GS. Typically, 0.73 ± 0.12 mg of GS with 20–30 % purity (based on SDS-PAGE) and 1010 ± 170 nmol/min/mg specific activity was obtained from 45–60 g of cell paste.

### Radioactive GS assays.

Reactions were initiated by mixing one volume of product entrapment-purified GS with one volume of 10 mM UDP-[U-$^{14}$C]Glc (specific activity ~800 cpm/nmol) in 2x assay buffer (150 mM Tris pH 7.5, 50 mM KF, 1.5 mM EDTA, 40 μM GTPγS and 1.5% BSA). The reactions were incubated at 30 °C, and an aliquot (5 μL) at each time point was quenched by mixing with 10% (w/v) TCA (100 μL) and passed through glass filters to collect insoluble glucan. The filters were washed three times with 10% (w/v) TCA (100 μL) followed by three times with EtOH (100 μL) and dried. To the filters were added 3 mL of scintillation fluid and radioactivity counted. The steady state kinetics parameters were determined in triplicate with different preparations of GS and the concentration of UDP-[U-$^{14}$C]Glc varied from 0.1 mM – 5 mM.

### Quantitation of UDP and Glc.

Assays were performed as described above using GS (8.0 μg/mL), 5 mM UDP-[U-$^{14}$C]Glc (specific activity ~800 cpm/nmol) in 145 μL of 1x assay buffer. At each time point, an aliquot (15 μL) was withdrawn and quenched by mixing with 84 μL 0.8% (w/v) perchloric acid. The solution was subsequently adjusted to pH ~6 with 21 μL of 0.5 M KOH, flash frozen and stored in −20 °C. Samples were thawed on ice and centrifuged at 20,000 g for 20 min. To remove CHS, 100 μL of $H_2O$ was added to 100 μL of the supernatant and extracted with 1 mL EtOAc. The mixture was separated by centrifugation at 20,000 *g* for 15 min and the EtOAc layer was removed. This extraction cycle was repeated three times, and after the third extraction, residual organic solvent was removed *in vacuo* using a SpeedVac. The

resulting aqueous solution was flash frozen and lyophilized overnight. The residue was dissolved in 100 μL of 20 mM ammonium acetate pH 6.0 and analyzed by HPAEC using a DNAPac PA100 column. Chromatography was performed using a gradient from 30 – 321 mM ammonium acetate pH 6.0 over 6 min at 30 °C and monitored by UV absorption of uridine. The pellet fraction of the quenched aliquots was resuspended in 100 μL of 5 mg/mL glucan from *Euglena gracilis* (Millipore Sigma) and transferred and filtered and washed on glass filters as described above to determine the amount of radioactive glucose incorporation by liquid scintillation counting.

### GS assays using HPAEC and SEC-PAD-RC.

GS reactions were performed under identical conditions as described above for the radioactive GS assay. At each time point, two aliquots were removed and quenched separately. One aliquot (5 μL) was quenched in 10% TCA (100 μL) and worked up as described above for radioactive GS assays to quantify the total amount of (1,3)-β-d-glucan. This analysis was used to confirm the quantitation by SEC-PAD-RC. For HPAEC and SEC analysis, the other aliquot (25 – 200 μL) was quenched by mixing with 5 – 10 equivalents of 2% (w/v) SDS and the mixtures were filtered through glass filters. To ensure complete removal of proteins and detergents, the filters were washed five times with 200 μL of 2% (w/v) SDS, five times with 200 μL $H_2O$ and five times with 200 μL EtOH. After drying under ambient conditions, the insoluble glucan was solubilized by sonicating the filters in 1 M NaOH (200 μL) in an ice/water bath for 10 min. The low temperature was important to minimize glucan hydrolysis. The mixture was centrifuged briefly, and 100 μL of the supernatant was withdrawn. The filter was resuspended in the remaining solution, centrifuged briefly, and ~80 uL of solution was recovered and combined with the first aliquot. The resulting mixture was centrifuged at 16,000 x g for 10 min at 4 °C to remove residual glass fibers. A small aliquot (5 μL) of the resulting supernatant was withdrawn, and the radioactivity was determined to quantify recovery of the solubilized glucan. Typical recoveries were 60–90%. The remaining supernatants were then analyzed by HPAEC or SEC analysis. For HPAEC, chromatography was performed using a CarboPac PA200 column and eluted with a convex curve gradient from 100 mM to 600 mM NaOAc in 100 mM NaOH over 50 min at a flow rate of 0.5 mL/min, followed by 1 M NaOAc in 100 mM NaOH for 15 min at a flow rate of 0.5 mL/min. The elution was fractionated every 3 min, and radioactivity determined by liquid scintillation counting (LSC). For SEC experiments, chromatography was performed on an Acclaim SEC-1000 column with 10 mM NaOH as an eluant with a flow rate of 0.3 mL/min. The elution was fractionated every 0.5 min between 5–15 min, and radioactivity determined by LSC. PAD traces for SEC experiments were scaled using a least squares fit approach to the RC data. We focused on the number averaged DP (Xn) because we observed change in the peak shape that decreased the peak maximum DP (Xp, Fig S3C) after long incubation times (> 20 min). The DP of the product was calculated based on the elution times of a commercial pullulan standard P-82 (Shodex Group) of defined Xp.

### SEC-PAD-RC analysis of GS products formed in the presence of UDP-Glc analogs.

GS assays were performed as described above for the $IC_{50}$ determination. The final concentrations of inhibitors in the reactions were 1 or 5 mM UDP-3’-dGlc, 2 or 10 mM

UDP-3'-F-Glc, 16 mM UDPcGlc, 100 μg/mL enfumafungin, or 10 μg/mL caspofungin. Reactions were incubated at 30 °C for 1 h, and were quenched and worked up for SEC-PAD-RC analysis.

## Results

### Purification and characterization of GS by product entrapment.

Endogenous GS was purified from *S. cerevisiae* due to the absence of a suitable heterologous expression system. As the difference in biochemical properties of the Fks1p and Fks2p subunits is unknown, we generated a *fks2Δ* strain for our GS preparation to avoid complications from functional heterogeneity, and all experiments were performed with this GS unless specified. Partial GS purification was achieved by product entrapment, exploiting GS affinity for its water-insoluble product (1,3)-β-D-glucan under turnover conditions [25]. The GS complex purified from the *fks2Δ* strain was 20 – 30% pure based on the SDS-PAGE band intensity analysis (Fig. 3, Fig. S1). The specific activity was 1010 ± 170 nmol $min^{-1}$ $mg^{-1}$ based on the incorporation of radioactive Glc from UDP-Glc into the water-insoluble (1,3)-β-D-glucan (Table S1). These values are comparable to those reported previously for *S. cerevisiae* GS purified with a mixture of Fks1p and Fks2p [25]. The co-purification of Fks1p and Rho1p was confirmed by Western blotting (Fig. 3, Fig. S1). As discussed later, Fks1p was also co-purified with Gas1p, suggesting a potential interaction between the two proteins.

The partially purified GS has $K_m$ = 0.37 ± 0.11 mM, consistent with the previous reports [26] and intracellular concentration of UDP-Glc in yeast (0.15 – 0.3 mM) [27]. The amount of UDP formation was stoichiometric to the amount of Glc incorporated into the insoluble (1,3)-β-D-glucan (Fig. 4). As the radioactive assays quantify only the water-insoluble (1,3)-β-D-glucan, the observations suggest that most, if not all, glucan products were water insoluble.

### Development of SEC-PAD-RC method to determine (1,3)-β-D-glucan glucan length.

While (1,3)-β-D-glucan is insoluble in water at neutral or acidic pH, it becomes soluble at pH > 11. Based on this unique property, we used a DIONEX liquid chromatography (LC) system, which allows chromatography at high pH and can detect carbohydrates using pulsed amperometric detection (PAD). As the previously reported average length of (1,3)-β-D-glucan produced by yeast GS is a 60 – 80-mer [6], we initially attempted to characterize the GS products using a CarboPac PA200 anion exchange column that could resolve partially hydrolyzed (1,3)-β-D-glucan with incremental lengths of up to ~80 Glc units (Fig. 5A). However, the (1,3)-β-D-glucan produced by GS eluted outside the limit of polymer length resolution (Fig. 5B), suggesting that the GS product is longer than 70-mer.

To address the resolution limit of the CarboPac PA200 column, we used an Acclaim SEC-1000 column for size exclusion chromatography (SEC). The column has a reported linear calibration range between 1 – 1,000 kDa (6–6,000 mer) of dextran. We also confirmed the linear range at the peak maximum (Xp) between 38 – 3,960 mer (Mp = 0.61 – 642 kDa) using pullulan (1,4-α-D-glucan) as a standard (Fig. S2). To analyze the GS product, GS assays were performed with UDP-[U-$^{14}$C]Glc, and the insoluble products were washed with

2% SDS, water and ethanol. The wash with 2% SDS was critical to remove any associated proteins that interfered with SEC analysis and detection with the PAD. The insoluble GS products were dissolved in 1 M NaOH and analyzed by SEC-PAD, and the eluent was fractionated for RC on a liquid scintillation counter. The two detection methods provided complementary information: PAD allows continuous monitoring, while RC allows accurate quantitation of Glc incorporation. These methods provided a robust approach of quantitative and sensitive detection of (1,3)-β-D-glucan without requiring any chemical modification. As shown in Fig. 5C, the chromatograms obtained from the two detection methods agree very well. The DP was determined by comparison to pullulan standards, which revealed the DP at the peak maximum (Xp) as 3,600 ± 220 (n = 3) for GS reactions with 5 mM UDP-Glc. The number and weight averaged DP (Xn and Xw respectively) were determined as 6,550 ± 760 and 12,300 ± 1,100, respectively, from which the polydispersity index (PDI) was determined as 2.8 ± 0.2. The length of (1,3)-β-D-glucan produced by GS was within the range of the reported DP of (1,3)-β-D-glucan isolated from the cell wall (1,500 – 8,000) [14], suggesting that the partially purified GS synthesizes (1,3)-β-D-glucan with physiologically relevant DP.

### (1,3)-β-D-glucan polymerization is processive.

To obtain kinetic insights into GS catalysis, GS reaction was quenched between 15 sec – 60 min and the product was characterized by SEC-PAD-RC. The resulting chromatograms (Fig. 6A) were analyzed to determine the polymer length at each time point (Fig. 6B, S3). Based on the glucan length and the total amount of glucose incorporation into glucan based on the radioactivity, the mole quantity of polymer molecules was calculated at each time point and plotted against incubation time (Fig. 6C). These analyses revealed a comprehensive picture of the timecourse kinetics of GS catalysis (Table 1). In the first minute, the glucan length increases linearly with very little change in the mole quantity of glucan. The mole quantity of glucan chains produced at 15 sec (10.2 ± 3.0 pmol) may be compared to the amount of Fks1p used in these assays (45 pmol; based on the purity determined by SDS-PAGE). These observations suggest that the first ~60 sec represents a pre-steady state where (1,3)-β-D-glucan is polymerized processively without being released from Fks1p. Thus, the rate of glucan elongation (number of glycosidic bonds formed by each GS per sec) was determined to be 51.5 ± 9.8 $sec^{-1}$ based on the slope of a linear fit to the data for the first 60 sec.

The glucan chain length reached its maximum at ~ 5 min, after which the length stayed constant with the mole quantity of polymer chain increasing linearly at least for 60 min (Fgi. 6C, Fig. S4), suggesting that the reaction is in a steady-state between 5 – 60 min. Between the pre-steady state and steady state, the total amount of Glc incorporated into glucan increased linearly without a burst or lag phase (Fig. S5), suggesting that the polymer elongation is the rate limiting step of the reaction. Therefore, the turnover rate of GS (mole quantity of glucan produced by each GS per min) can be deduced by dividing the length of glucan during the steady state by the elongation rate (51.5 ± 9.8 $sec^{-1}$), which resulted in 0.47 ± 0.11 $min^{-1}$ (Table 1). These analyses suggest that GS catalyzes formation of multiple glucan chains, and provide strong evidence that GS releases the (1,3)-β-D-glucan products and re-initiates polymerization of a new glucan chain.

### (1,3)-β-D-glucanosyltransferase is not essential for the production of glucan with a physiological length.

Since our preparation does not provide homogeneously purified GS, we considered a possibility of contaminating enzyme activities that could change the length or kinetics of glucan formation. Thus, we first tested for glucosidase activity by incubating enzymatically prepared (1,3)-β-D-[$^{14}$C]glucan with the purified GS. No change in the length was observed by SEC-PAD-RC and no release of radioactive material was observed even after 3 h incubation (Fig. S6), demonstrating the absence of any detectable level of contaminating enzyme activities that could alter the length of glucan in the time scale relevant to our assays.

Furthermore, we characterized the purified GS by MS after trypsin digestion. This analysis confirmed that FKS1 was the most abundant protein. Three enzymes, Gas1p, Gas5p, and Bgl2p, functionally related to (1,3)-β-D-glucan biosynthesis or remodeling were detected with low abundance. Among these, Gas1 and Gas5 were the only enzymes reported to have in vitro activity to catalyze elongation of (1,3)-β-D-glucan length. Bgl2 catalyzes β-(1,6)-branching and does not catalyze β-(1,3)-elongation [11]. The presence of Gas1p was also confirmed by Western blotting (Fig. 3, Fig. S7).

While Gas1p and Gas5p have similar in vitro activities [28], Gas1p has been proposed to be responsible for β-(1,3)-elongation in vivo. Furthermore, quantitation based on mass spectrum counts [29] suggested that Gas1p is much more abundant than Gas5p in our GS preparation. Therefore, we investigated if Gas1p is involved in the in vitro formation of (1,3)-β-D-glucan using GS from *S. cerevisiae* BY4741 *gas1Δ* (ΔGas1-GS). The ΔGas1-GS was prepared by the product entrapment approach with comparable purity (25 %) except for the absence of Gas1p at 125 kDa (Fig. 3). The specific activity (877 nmol min$^{-1}$ mg$^{-1}$ GS) was also comparable to that of GS containing Gas1p. Timecourse assays of ΔGas1-GS revealed that the elongation rate of 42.3 ± 5.9 sec$^{-1}$ and the steady-state glucan DP (Xn) of 5100 ± 310, which are similar to those in the presence of Gas1p (Table 1, Fig. 7 and S3), suggesting minimal to no effects of Gas1p on the elongation rate or overall length of (1,3)-β-D-glucan produced in vitro. Based on these observations, GS with Fks1p is likely sufficient for the formation of (1,3)-β-D-glucan with the physiologically relevant DP. The absence of effects of Gas1p on the glucan length is also consistent with the rate of GS catalysis (51.5 sec$^{-1}$), which was > 100 folds faster than the reported rate of any of the glucanosyltransferases including Gas1p (< 0.5 sec$^{-1}$). Gas1p is likely involved in the branching and side-chain elongation of the Fks1p product forming mature cell wall components.

### Effects of UDP-Glc, potential priming substrates, and antifungals on chain length.

To determine the potential factors governing length specificity of GS, we determined the length of GS products formed in assays with varying concentrations of UDP-Glc, with putative priming substrates, or with antifungal GS inhibitors. The assays were performed with UDP-Glc at concentrations close to (0.5 mM), below (0.1 mM) or above (5 mM) the $K_m$ value (Fig. 8A, 8B, and S7A). Within the physiologically relevant range of UDP-Glc (0.15 – 0.3 mM), UDP-Glc concentrations have minimal effects on the glucan length. While

the Xp in all three conditions was similar, statistically significant differences in the Xw and Xn for the glucan formed in these assays were observed between 0.1 and 5 mM UDP-Glc which may suggest that the length of GS products is determined by a process whose kinetics is affected by substrate binding.

If GS catalyzes the non-reducing end polymerization, monomeric D-Glc or short (1,3)-β-D-glucan oligomers may serve as priming substrates, as was observed for chitin synthase [17]. Thus, we investigated the effects of D-Glc and laminaribiose (Lam) on the GS products were investigated. Even at 10 mM, neither D-Glc nor Lam significantly affected the (1,3)-β-D-glucan length (Fig. 8C, 8D, and S7B). These observations are in contrast to the effect of GlcNAc on the chitin synthase activity, where the presence of GlcNAc increased the activity of chitin synthase, and induced the formation of short chitooligosaccharides [17]. The distinct effects of monomers on GS and chitin synthase suggest distinct mechanisms of initiation between the two enzymes.

GS is non-competitively inhibited by three structurally distinct classes of antifungal antibiotics (Fig. 1B). However, the details of their mechanism of inhibition, whether they are inhibiting the overall activity of GS or affecting the length of GS products, is not known. To obtain insights into the mechanism of inhibition, we investigated the length of glucan formed in the presence of caspofungin (CFN) and enfumafungin (ENF). The $IC_{50}$ values for CFN and ENF were determined as 0.26 ± 0.06 and 7.1 ± 2.6 μg/mL respectively (Fig. S8C), which are comparable to those reported previously [30, 31]. To determine the effects of the antifungals on the length of GS product, GS assays were performed in the presence of the antifungals at concentrations >10 fold above the $IC_{50}$ value to ensure maximum inhibition. Even with such high concentrations of antifungals, no change in the glucan length was observed (Fig. 8E, 8F, S7D). These observations suggest that these antifungals inhibit the overall activity of GS without altering the length of the (1,3)-β-D-glucan product.

### GS catalyzes non-reducing end polymerization.

The direction of polymerization of GS cannot be studied by approaches most frequently used to determine the direction of polymerization by polysaccharide synthases. Therefore, we used 1’- and 3’-blocked UDP-Glc analogs in combination with the SEC-PAD-RC method. If the elongation proceeds at the non-reducing end, the 3’-blocked analogs are expected to serve as chain terminators, cause premature termination and form shorter glucan (Fig. 2A). On the other hand, if the elongation proceeds at the reducing end, the 1’-blocked analogs will serve as the chain terminator (Fig. 2B). Thus, by studying the length of GS products in the presence of these substrate analogs, the direction of polymerization can be determined unambiguously.

For the 1’-blocked analog, we synthesized a phosphonate analog of UDP-Glc, UDPcGlc (Fig. 2A), which has a C-C bond at the anomeric position that cannot be cleaved by a glycosyltransferase, and hence cannot serve as a sugar donor. For the 3’-blocked analog, we initially synthesized UDP-3’-fluoroglucose (UDP-3’-F-Glc, Fig. 2B) which does not have a nucleophile at the 3’-position and thus cannot serve as a sugar acceptor. These blocked UDP-Glc analogs were prepared chemoenzymatically. Facile synthesis was achieved by employing enzymatic nucleotidylation of sugar 1-phosphate analogs using the *E. coli* UDP-

Glc pyrophosphorylase GalU. Using this approach, UDPcGlc was prepared from D-glucose-1-phosphonate with an isolation yield of 34% and UDP-3'-F-Glc was prepared from 3-deoxy-3-fluoroglucose 1-phosphate with an isolation yield of 47%.

UDPcGlc and UDP-3'-F-Glc both inhibited the GS activity with $IC_{50}$ values of 2.8 ± 0.3, and 5.3 ± 1.0 mM (Fig. 9A), respectively, which are slightly higher than the 1 mM UDP-Glc used in these assays. The effects of these analogs on product lengths were determined by performing assays in the presence of both UDP-Glc and one of the blocked analogs at ~ half of $IC_{50}$ or > 2 folds above $IC_{50}$ (Fig. 9B, and 9C). The assays were incubated for 60 min to monitor the effects during the steady state. With addition of UDPcGlc, the length of the GS product was not altered and only the total amount of polymer decreased (Fig. 9B). In contrast, in assays with UDP-3'-F-Glc, the length of the polymer products was significantly shortened in response to the increased concentrations of the analog (Fig. 9B, and S8). As the observed effect of UDP-3'-F-Glc could be caused by the reduced reactivity of the anomeric position due to an electron withdrawing fluorine at the 3'-position, the effect of another 3'-blocked analog, UDP-3'-deoxyglucose (UDP-3'-dGlc, Fig. 2B), was investigated. UDP-3'-dGlc was synthesized as above with 38% isolation yield and inhibited GS with an $IC_{50}$ value of 2.4 ± 0.2 mM (Fig. 9A). When we investigated the length of GS products formed in the presence of UDP-3'-dGlc by SEC-PAD-RC, UDP-3'-dGlc was found to shorten the GS products in response to increasing concentrations of UDP-3'-dGlc, similar to UDP-3'-F-Glc (Fig. 9B, 9C, and S8). These observations suggest that the observed shortening of glucan polymer in the presence of the 3'-blocked analogs was caused by the absence of a nucleophilic functional group at the 3'-position of the UDP-Glc analogs, thus preventing glucan elongation (Fig. 2B). Therefore, our observations are most consistent with non-reducing end polymerization.

## Discussion

This study describes mechanistic characterization of *S. cerevisiae* GS using our newly developed SEC-based assay method that allows quantitative characterization of (1,3)-β-D-glucan. GS is a proven target of antifungals and a key enzyme in fungal cell wall biosynthesis. Despite the importance of GS, its mechanism is largely uninvestigated due to challenges in characterizing the insoluble (1,3)-β-D-glucan product. This is a common problem in many biopolymer biosynthesis enzymes, where the absence of suitable assay methods limits our understanding of the enzymes' mechanisms. In the case of GS, the (1,3)-β-D-glucan product is charge neutral and insoluble at neutral pH. As a result, no quantitative method of characterization was available to determine the length and amount with throughput suitable for enzyme activity assays. While reducing end quantification has been used to determine the length of GS products [6], the application of this approach to mechanistic studies is not practical due to the large amount of materials needed (normally in mmol quantity). Also, the method only reports average values without dispersity information. Our method overcomes these issues. The assay involves relatively simple workup and usually requires only 25 – 200 μL of the assay solution. The lower limit of detection is 100 pmol of Glc. Due to this robustness, our method allowed for the mechanistic characterization of yeast GS with unprecedented detail.

Our SEC-PAD-RC analysis revealed that the partially purified GS produces (1,3)-β-D-glucan with Xn of 2,000 – 7,000 depending on concentration of UDP-Glc. Previously, yeast GS in crude membrane preparations was reported to produce 60 – 80 mer glucan polymer based on reducing end quantification [6]. The most likely cause of the discrepancy is the method of characterization. The reducing end quantitation requires extensive work-up, in which the reducing end of the polysaccharide is chemically reduced, followed by hydrolysis of the polymer and quantitation of the ratio of the non-reducing and reducing sugars. The chemical reduction requires harsh conditions where partial degradation is unavoidable, and the method is inherently sensitive to minor degradation. In fact, when we repeated the reducing end quantitation, we observed significant variations in the results depending on the concentration of NaOH used to solubilize (1,3)-β-D-glucan, suggesting substantial cleavage of (1,3)-β-D-glucan under these conditions. Additionally, characterization of long polysaccharides by reducing end quantitation is challenging because of the low abundance of the free reducing end compared to the total sugars in the polysaccharide. In contrast, our SEC-PAD-RC approach determines the length and amounts of polymer produced with no modification of the product, which minimizes the amount and effect of degradation of (1,3)-β-D-glucan. The method also offers highly sensitive detection; each assay needs ~100 pmol of Glc with radioactivity of ~1 x $10^3$ cpm/μmol, approximately 3 orders of magnitude less compared to 1 μmol of Glc with 4.4 x $10^6$ cpm/μmol required for the reducing end quantitation [6]. Thus, the SEC-PAD-RC method allows sensitive and accurate characterization of GS products, and revealed that GS produces (1,3)-β-D-glucan with the length much longer than previously reported and more consistent with the length of (1,3)-β-D-glucan purified from the cell wall.

The production of (1,3)-β-D-glucan with the length of 6,550 ± 760 mer suggests that GS alone forms the linear (1,3)-β-D-glucan precursor for cell wall biosynthesis. We observed the co-purification of the (1,3)-β-D-glucanosyltransferase Gas1p previously proposed to be responsible for the (1,3)-β-D-glucan elongation (Fig. 1A, path A) suggesting a potential interaction between Gas1p and Fks1p. However, the characterization of ΔGas1-GS suggests that Gas1p has minimal to no role in the formation of the linear (1,3)-β-D-glucan in vitro. Furthermore, the rate of (1,3)-β-D-glucan elongation by GS (51.5 $sec^{-1}$) is > 100-folds greater than the previously reported rates of (1,3)-β-D-glucan transfer catalyzed by (1,3)-β-D-glucanosyltransferases (0.17 – 0.48 $sec^{-1}$) [32]. These observations are inconsistent with the model where GS catalyzes short glucan that is then elongated by (1,3)-β-D-glucanosyltransferases (Fig. 1A, path A), but more consistent with the model where GS alone is sufficient for formation of the long linear (1,3)-β-D-glucan that is subsequently modified by (1,3)-β-D-glucanosyltransferases (Fig. 1A, path B). Therefore, observations described here provide quantitative evidence for the functional relationship between GS and (1,3)-β-D-glucanosyltransferases and provide clearer understanding of the early steps in the fungal cell wall biosynthesis.

Our SEC-PAD-RC method also provided quantitative insights into the catalytic mechanism of GS. The timecourse assays revealed the highly processive elongation of (1,3)-β-D-glucan without formation of short oligosaccharides. Based on the elongation rate of ~50 Glc $sec^{-1}$, GS is expected to produce one polymer chain every ~1–2 min for more than 60 min. These observations suggest that each Fks1p forms multiple chains of (1,3)-β-D-glucan, and that GS

releases the polymer product and re-initiates the polymerization. The presence of the termination and re-initiation steps is consistent with the ability to purify catalytically active GS through product entrapment, where GS is bound to insoluble (1,3)-β-D-glucan under turnover conditions and released in the absence of substrate.

This kinetic characterization of GS catalysis suggested that the direction of polymerization of GS cannot be studied by common approaches used to determine the direction of polymerization by polysaccharide synthases. The absence of the knowledge in the mechanism of initiation makes it impossible to use priming substrates or its analogs, and the rapid kinetics make it difficult to perform informative pulse-chase experiments. Therefore, we characterized the direction of polymerization by using 1'- and 3'-blocked substrate analogs in combination with our SEC-PAD-RC assay method. The activity assays in the presence of the 3'-blocked analogs resulted in the formation of shorter glucan polymers while the 1'-blocked analog did not alter the product length, which were most consistent with the non-reducing end polymerization.

Based on these mechanistic characterizations, we propose a model for the GS catalytic cycle (Fig. 10) consisting of three major steps; initiation, elongation and termination. The polymerization is initiated by self-priming of GS with UDP-Glc in the absence of exogenously added priming substrate. The mechanism and nature of the initiation step is currently unknown. Unlike chitin synthase, Glc or short oligosaccharides do not serve as priming substrates. One possibility is that GS catalyzes a hydrolysis of UDP-Glc and the resulting Glc is used as priming substrate without its release into the solution. Such mechanism has been proposed for cellulose synthase [33]. Alternatively, the Glc may be transferred to a co-purified short glucan oligomer or lipid, from which the glucan chain elongates. Subsequent elongation step proceeds by adding Glc at the non-reducing end of the nascent chain at the rate of ~50 $sec^{-1}$. When the polymer length reaches 6,550 ± 760 mer, the product is released from the enzyme and the initial state of the enzyme is regenerated. The length specificity is likely an inherent property of the enzyme as it is minimally affected by substrate and not at all by inhibitors. Since we observed the pre-steady state chain elongation in the first ~2 min with no lag or burst phase in the rate of D-Glc incorporation into glucan, the rate determining step is likely the elongation step.

This study highlights the significance of quantitative characterization of the length and amount of polymer products in understanding the functions and mechanism of GS in fungal cell wall biosynthesis. The study provides a clearer view of the function of GS in the fungal cell wall biosynthesis, and quantitative insights into the catalytic mechanism of GS. The length determination in combination with the blocked substrate analogs provides a powerful approach to unambiguously determine the direction of polymerization. This approach can be generally applied to many polysaccharide biosynthesis enzymes regardless of the mechanisms of initiation, or length specificity, allowing mechanistic and functional characterization of these enzymes.

## Supplementary Material

Refer to Web version on PubMed Central for supplementary material.

## ACKNOWLEDGMENT

We thank Tricia Ho and Dr. Erik Soderblom in the Duke University School of Medicine Proteomics and Metabolomics facility for LC-MS/MS characterization of GS. We also acknowledge the Duke University NMR Spectroscopy Center shared resource for spectrometer time. We thank Dr. Yoichi Noda at the University of Tokyo and Dr. Randy Shekman at University of California Berkeley for sharing anti-Gas1p antibody, Dr. Yoshikazu Ohya for anti-Rho1p antibody, and Dr. Jean-Paul Latgé at the Institut Pasteur for anti-FKS antibody.

Funding Sources

This work was supported by the Duke University Medical Center, National Institute of General Medical Sciences R01 GM115729 (to K.Y.). A.L. was supported by the Tri-Institutional Molecular Mycology and Pathogenesis Training Program from National Institute of Allergy and Infectious Disease (T32AI052080). NMR instruments in the Duke University NMR Spectroscopy Center was purchased with support from NIH, NSF, HHMI and the North Carolina Biotechnology Center.

## ABBREVIATIONS

| | |
|---|---|
| **GS** | (1,3)-β-D-glucan synthase |
| **HPAEC** | high performance anion exchange chromatography |
| **PAD** | pulsed-amperometric detection |
| **RC** | radiation counting |

## REFERENCES

[1]. Latge J-P, and Steinbach WJ (2009) Aspergillus fumigatus and Aspergillosis, ASM Press, Washington, DC.

[2]. Roemer T, and Krysan DJ (2014) Antifungal drug development: challenges, unmet clinical needs, and new approaches, Cold Spring Harb Perspect Med 4, a019703. [PubMed: 24789878]

[3]. Orlean P (2012) Architecture and biosynthesis of the Saccharomyces cerevisiae cell wall, Genetics 192, 775–818. [PubMed: 23135325]

[4]. Munro CA (2013) Chitin and glucan, the yin and yang of the fungal cell wall, implications for antifungal drug discovery and therapy, Adv Appl Microbiol 83, 145–172. [PubMed: 23651596]

[5]. Douglas CM (2001) Fungal beta(1,3)-D-glucan synthesis, Medical mycology 39 Suppl 1, 55–66. [PubMed: 11800269]

[6]. Shematek EM, Braatz JA, and Cabib E (1980) Biosynthesis of the yeast cell wall. I. Preparation and properties of beta-(1 leads to 3)glucan synthetase, J Biol Chem 255, 888–894. [PubMed: 6766139]

[7]. Ishihara S, Hirata A, Nogami S, Beauvais A, Latge JP, and Ohya Y (2007) Homologous subunits of 1,3-beta-glucan synthase are important for spore wall assembly in Saccharomyces cerevisiae, Eukaryot. Cell 6, 143–156. [PubMed: 17158736]

[8]. Zhao C, Jung US, Garrett-Engele P, Roe T, Cyert MS, and Levin DE (1998) Temperature-induced expression of yeast FKS2 is under the dual control of protein kinase C and calcineurin, Mol Cell Biol 18, 1013–1022. [PubMed: 9447998]

[9]. Manners DJ, Masson AJ, and Patterson JC (1973) The structure of a beta-(1 leads to 3)-D-glucan from yeast cell walls, Biochem J 135, 19–30. [PubMed: 4359920]

[10]. Muller A, Ensley H, Pretus H, McNamee R, Jones E, McLaughlin E, Chandley W, Browder W, Lowman D, and Williams D (1997) The application of various protic acids in the extraction of (1->3)-beta-D-glucan from Saccharomyces cerevisiae, Carbohydr Res 299, 203–208. [PubMed: 9163899]

[11]. Aimanianda V, Simenel C, Garnaud C, Clavaud C, Tada R, Barbin L, Mouyna I, Heddergott C, Popolo L, Ohya Y, Delepierre M, and Latge JP (2017) The Dual Activity Responsible for the

Elongation and Branching of beta-(1,3)-Glucan in the Fungal Cell Wall, Mbio 8, e00619–00617. [PubMed: 28634239]

[12]. Gastebois A, Fontaine T, Latgé J-P, and Mouyna I (2010) beta(1–3)Glucanosyltransferase Gel4p Is Essential for Aspergillus fumigatus, Eukaryot. Cell 9, 1294–1298. [PubMed: 20543062]

[13]. de Medina-Redondo M, Arnaiz-Pita Y, Clavaud C, Fontaine T, del Rey F, Latge JP, and de Aldana CRV (2010) beta(1,3)-Glucanosyl-Transferase Activity Is Essential for Cell Wall Integrity and Viability of Schizosaccharomyces pombe, PLoS One 5, e14046. [PubMed: 21124977]

[14]. Mouyna I, Hartl L, and Latgé J-P (2013) beta-1,3-glucan modifying enzymes in Aspergillus fumigatus, Front Microbiol 4, 81. [PubMed: 23616783]

[15]. Cabib E, Blanco N, and Arroyo J (2012) Presence of a Large beta(1–3)Glucan Linked to Chitin at the Saccharomyces cerevisiae Mother-Bud Neck Suggests Involvement in Localized Growth Control, Eukaryot. Cell 11, 388–400. [PubMed: 22366124]

[16]. Ram AFJ, Kapteyn JC, Montijn RC, Caro LHP, Douwes JE, Baginsky W, Mazur P, Van den Ende H, and Klis FM (1998) Loss of the plasma membrane-bound protein Gas1p in Saccharomyces cerevisiae results in the release of beta 1,3-glucan into the medium and induces a compensation mechanism to ensure cell wall integrity, J Bacteriol 180, 1418–1424. [PubMed: 9515908]

[17]. Gyore J, Parameswar AR, Hebbard CF, Oh Y, Bi E, Demchenko AV, Price NP, and Orlean P (2014) 2-acylamido analogues of N-acetylglucosamine prime formation of chitin oligosaccharides by yeast chitin synthase 2, J Biol Chem 289, 12835–12841. [PubMed: 24619411]

[18]. Weigel PH, West CM, Zhao P, Wells L, Baggenstoss BA, and Washburn JL (2015) Hyaluronan synthase assembles chitin oligomers with -GlcNAc(alpha 1 - >)UDP at the reducing end, Glycobiology 25, 632–643. [PubMed: 25583822]

[19]. Tlapak-Simmons VL, Baron CA, Gotschall R, Haque D, Canfield WM, and Weigel PH (2005) Hyaluronan biosynthesis by class I streptococcal hyaluronan synthases occurs at the reducing end, J. Biol. Chem 280, 13012–13018. [PubMed: 15668242]

[20]. Mukerjea R, and Robyt JF (2005) Starch biosynthesis: further evidence against the primer nonreducing-end mechanism and evidence for the reducing-end two-site insertion mechanism, Carbohydr Res 340, 2206–2211. [PubMed: 16026770]

[21]. Larson ME, Falconer DJ, Myers AM, and Barb AW (2016) Direct Characterization of the Maize Starch Synthase IIa Product Shows Maltodextrin Elongation Occurs at the Non-reducing End, J. Biol. Chem 291, 24951–24960. [PubMed: 27733678]

[22]. Huh WK, Falvo JV, Gerke LC, Carroll AS, Howson RW, Weissman JS, and O'Shea EK (2003) Global analysis of protein localization in budding yeast, Nature 425, 686–691. [PubMed: 14562095]

[23]. Goldstein AL, and McCusker JH (1999) Three new dominant drug resistance cassettes for gene disruption in Saccharomyces cerevisiae, Yeast 15, 1541–1553. [PubMed: 10514571]

[24]. Agatep R, Kirkpatrick RD, Parchaliuk DL, Woods RA, and Gietz RD (1998) Transformation of Saccharomyces cerevisiae by the lithium acetate/single-stranded carrier DNA/polyethylene glycol protocol, Technical Tips Online 3, 133–138.

[25]. Inoue SB, Takewaki N, Takasuka T, Mio T, Adachi M, Fujii Y, Miyamoto C, Arisawa M, Furuichi Y, and Watanabe T (1995) Characterization and Gene Cloning of 1,3-Beta-D-Glucan Synthase from Saccharomyces-Cerevisiae, Eur J Biochem 231, 845–854. [PubMed: 7649185]

[26]. Okada H, Abe M, Asakawa-Minemura M, Hirata A, Qadota H, Morishita K, Ohnuki S, Nogami S, and Ohya Y (2010) Multiple functional domains of the yeast 1,3-beta-glucan synthase subunit Fks1p revealed by quantitative phenotypic analysis of temperature-sensitive mutants, Genetics 184, 1013–1024. [PubMed: 20124029]

[27]. Gancedo JM, and Gancedo C (1973) Concentrations of Intermediary Metabolites in Yeast, Biochimie 55, 205–211. [PubMed: 4578278]

[28]. Ragni E, Fontaine T, Gissi C, Latge JP, and Popolo L (2007) The Gas family of proteins of Saccharomyces cerevisiae: characterization and evolutionary analysis, Yeast 24, 297–308. [PubMed: 17397106]

[29]. Ishihama Y, Oda Y, Tabata T, Sato T, Nagasu T, Rappsilber J, and Mann M (2005) Exponentially modified protein abundance index (emPAI) for estimation of absolute protein amount in proteomics by the number of sequenced peptides per protein, Mol Cell Proteomics 4, 1265–1272. [PubMed: 15958392]

[30]. Onishi J, Meinz M, Thompson J, Curotto J, Dreikorn S, Rosenbach M, Douglas C, Abruzzo G, Flattery A, Kong L, Cabello A, Vicente F, Pelaez F, Diez MT, Martin I, Bills G, Giacobbe R, Dombrowski A, Schwartz R, Morris S, Harris G, Tsipouras A, Wilson K, and Kurtz MB (2000) Discovery of novel antifungal (1,3)-beta-D-glucan synthase inhibitors, Antimicrob Agents Chemother 44, 368–377. [PubMed: 10639364]

[31]. Douglas CM, Marrinan JA, Li W, and Kurtz MB (1994) A Saccharomyces-Cerevisiae Mutant with Echinocandin-Resistant 1,3-Beta-D-Glucan Synthase, J Bacteriol 176, 5686–5696. [PubMed: 8083161]

[32]. Hartland RP, Fontaine T, Debeaupuis JP, Simenel C, Delepierre M, and Latge JP (1996) A novel beta-(1–3)-glucanosyltransferase from the cell wall of Aspergillus fumigatus, J. Biol. Chem 271, 26843–26849. [PubMed: 8900166]

[33]. McManus JB, Yang H, Wilson L, Kubicki JD, and Tien M (2018) Initiation, Elongation, and Termination of Bacterial Cellulose Synthesis, Acs Omega 3, 2690–2698. [PubMed: 30023847]

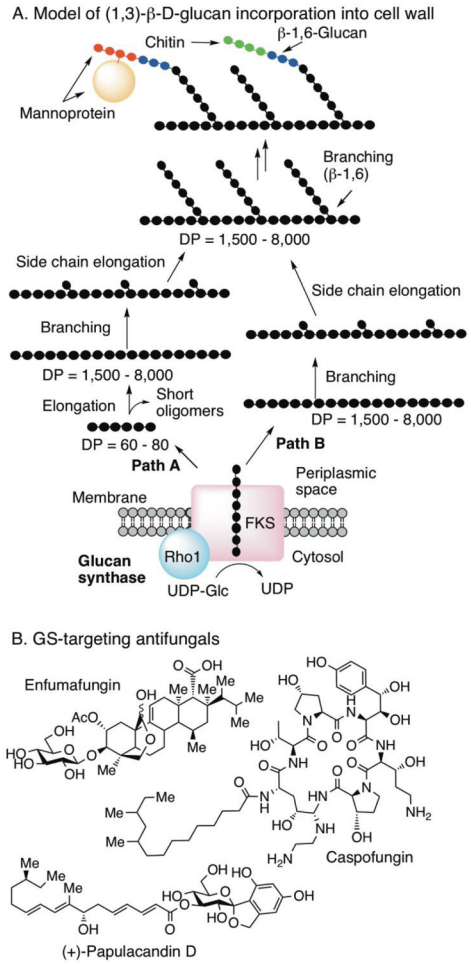


**Figure 1.**

Proposed mechanisms of fungal cell wall biosynthesis and GS-targeting antifungal agents. (A) Schematic representation of the (1,3)-β-D-glucan biosynthesis and its integration into the fungal cell wall. GS could catalyze formation of either relatively short (1,3)-β-D-glucan that requires subsequent elongation by actions of (1,3)-β-d-glucanosylases (path A), or full length (1,3)-β-D-glucan that is directly used for branching and side chain elongation (path B). The linear (1,3)-β-D-glucan formed by GS is extruded to the periplasmic space, where (1,3)-β-D-glucanosylases are available for further modification. The GS complex is composed of Rho1p GTPase (blue circle) and Fks1p catalytic subunit (pink rectangle). (1,3)-β-D-glucan is shown in black, (1,6)-β-D-glucan in blue, chitin in green and mannoproteins in red/yellow. (B) Structures of representative members of the three classes of GS-targeting antifungals.

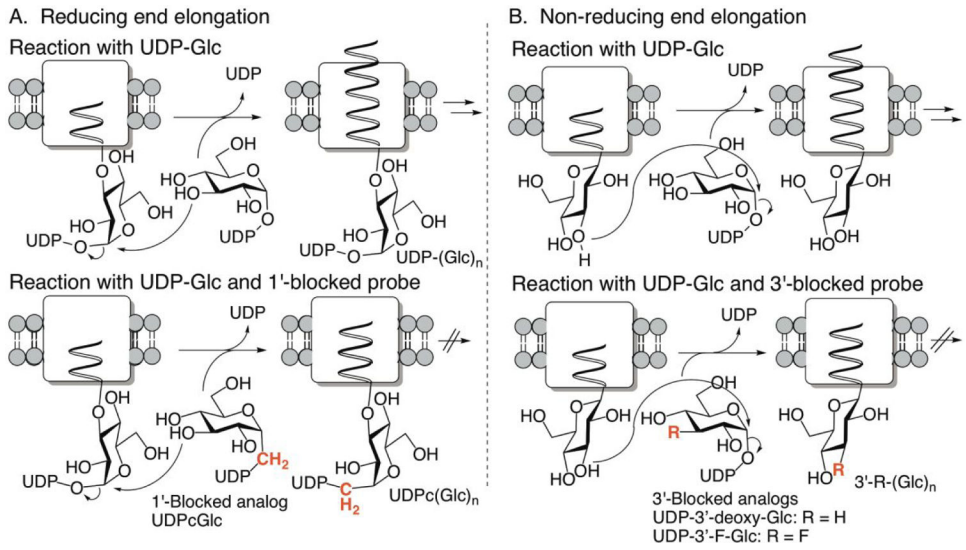


**Figure 2.**

Two possible directions of (1,3)-β-D-glucan elongation by GS. Shown are the reducing end (*A*) and non-reducing end (*B*) polymerization models of (1,3)-β-D-glucan, and the expected mechanism-based premature termination by 1'- and 3'-blocked UDP-Glc analogs. The analogs are expected to be incorporated into the nascent chain, but because they carry chemically inert functional group at the 1'- or 3'-position, subsequent elongation will not occur, forcing termination of glucan polymerization.

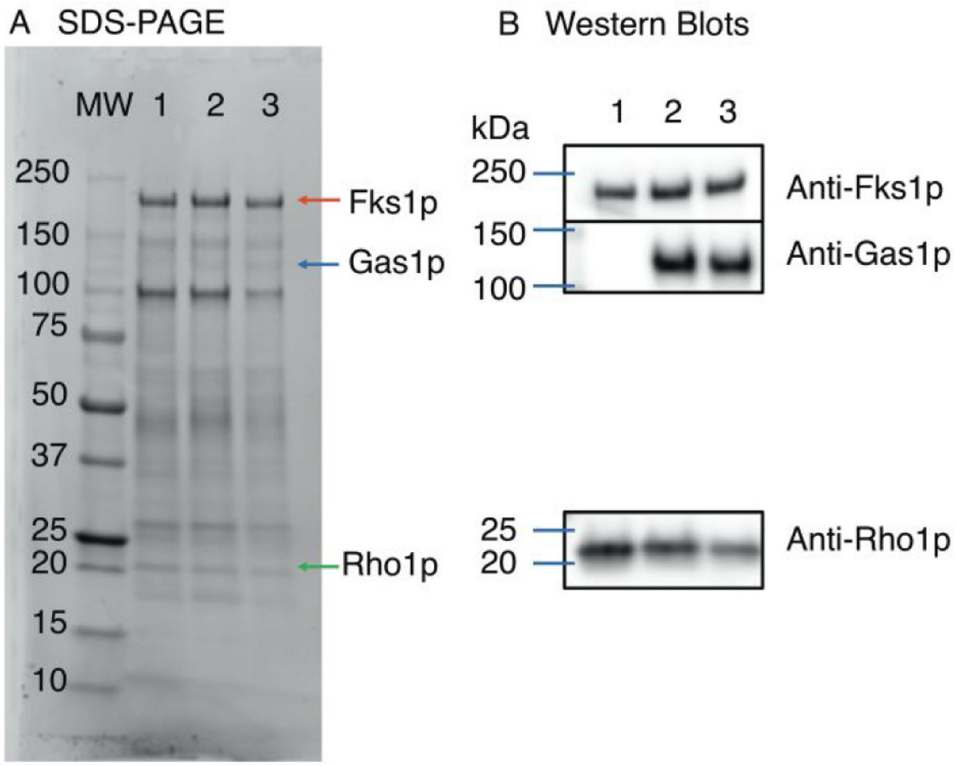


**Figure 3.**

Characterization of partially purified GS by SDS-PAGE (A) and Western blotting (B). Lanes: 1, ΔGas1-GS; 2, ΔFks2-GS; 3, BY4741-GS. The Western blotting was performed with anti-FKS, anti-Rho1p, or anti-Gas1p antibody. Images of the Western blot with the entire molecular weight range are shown in Fig. S7.

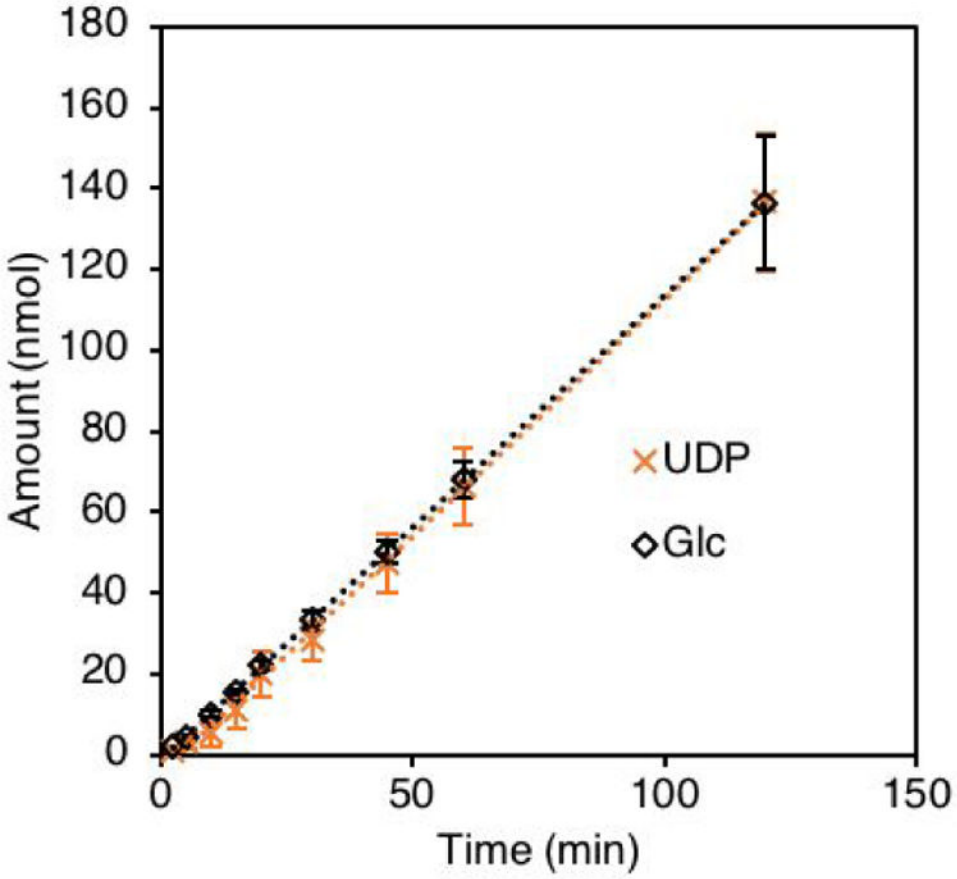


**Figure 4.**

Stoichiometry of the GS reaction. UDP release is equal to the amount of Glc incorporated into insoluble (1,3)-β-D-glucan. Experiments were performed in triplicate, and error bars represent standard deviation (SD).

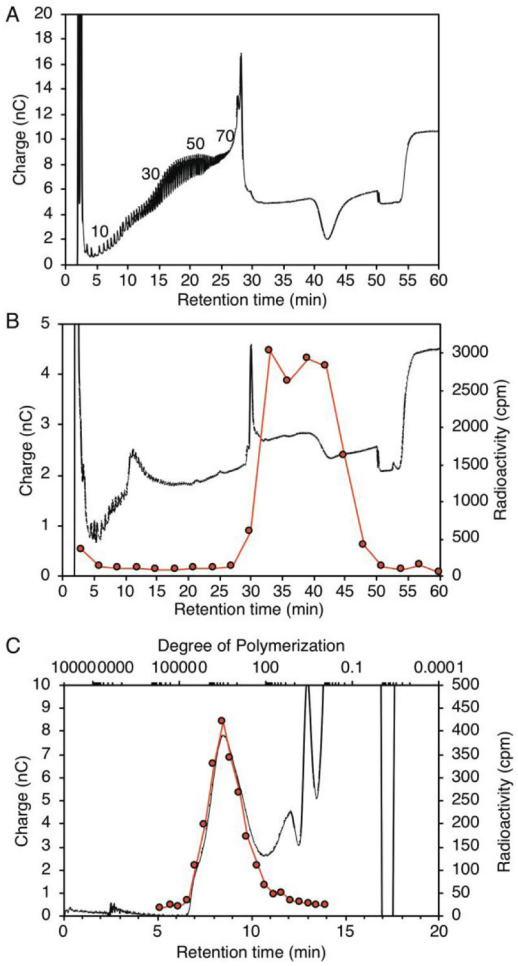


**Figure 5.**

Characterization of GS products by HPAEC or SEC. (A and B) Analysis of partially hydrolyzed (1,3)-β-D-glucan standard (A) or GS reaction product (B) using a CarboPac PA200 column. More than 95% of radioactivity from GS reaction products eluted in the region longer than expected for ~70-mer (1,3)-β-D-glucan. (C) SEC analysis of GS reaction product using an Acclaim SEC-1000 column. The chromatograms from electrochemical detection is shown as a solid trace in black and radioactivite quantitation in red circles.

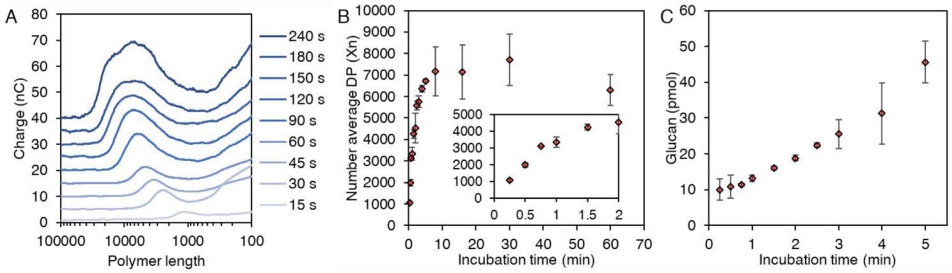


**Figure 6.**

Time course analysis of the GS reaction by SEC-PAD-RC. (*A*) Representative chromatograms of SEC-PAD for early timepoints quenched between 15 – 240 sec. (*B*) The length of (1,3)-β-D-glucan formed during GS assays. The number averaged DP of (1,3)-β-D-glucan (Xn) was plotted against incubation time. The inset shows a zoomed in view of the first 2 min of the reaction. (*C*) The number of glucan polymer chains in moles produced during the course of GS assays. The mole quantity of glucan chain was calculated based on total radioactive glucose incorporation divided by Xn. In *B* and *C*, each data point represents an average of three replicates, and the error bars represent standard deviation (SD).

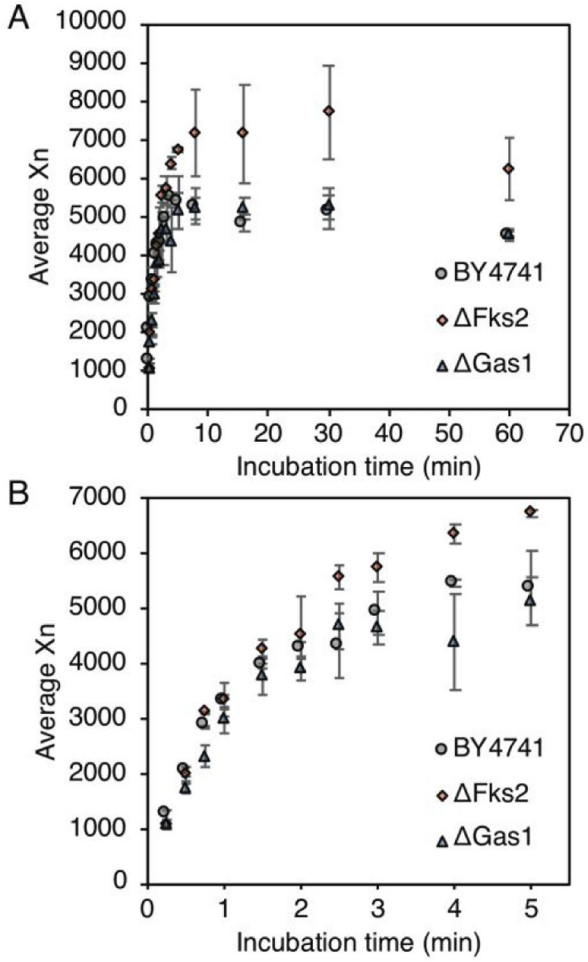


**Figure 7.**

Degree of polymerization (DP) of (1,3)-β-D-glucan produced by BY4741-GS, ΔFks2-GS, and ΔGas1-GS. Shown are number average DP (Xn) calculated from SEC-PAD-RC analysis. Experiments were performed in triplicate, and error bars represent ±1 SD around the mean. (B) is a magnified view of (A).

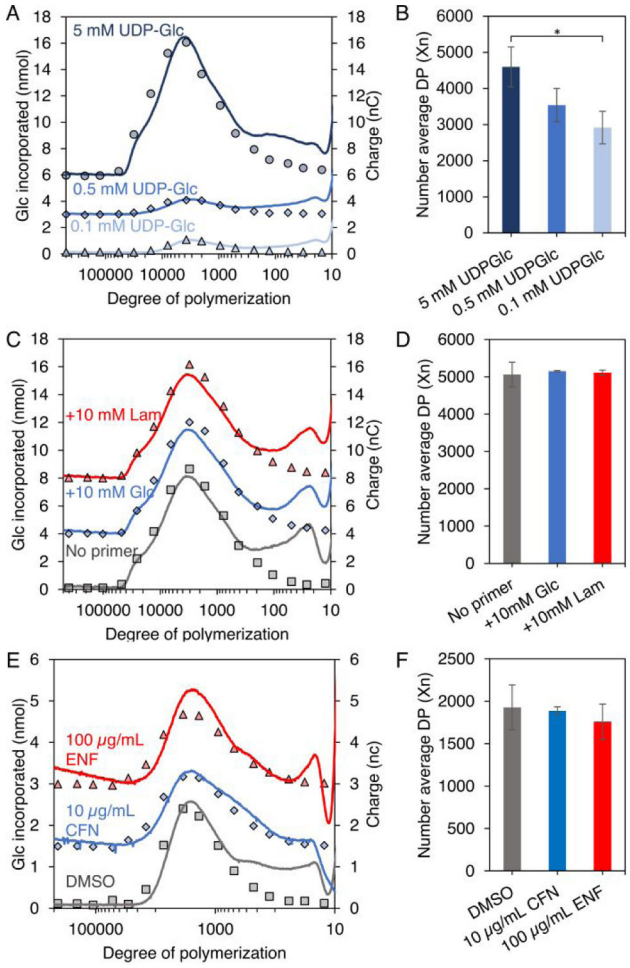


**Figure 8.**

Effects on glucan length of substrate concentration, Glc, Lam, and antifungal GS inhibitors. Shown are representative SEC-PAD-RC chromatograms (*A*, *C*, and *E*) and the number average DP (Xn) of GS products (*B*, *D*, and *F*) in assays with different concentrations of UDP-Glc (*A* and *B*), with potential priming substrates (*C* and *D*), and with antifungal GS inhibitors (*E* and *F*). In *A*, *C*, and *E*, the RC quantitation of (1,3)-β-D-glucan is shown as individual data points for each fraction (left axis), and the scaled PAD chromatograms are shown in solid lines (right axis). In *A*, five times more material was analyzed for the 0.1 mM UDP-Glc reaction, compared to 0.5 and 5 mM UDP-Glc reactions. Data in *B*, *D*, and *F* represents an average of three replicates, and error bars represent SD. *P* values were calculated using t-tests to compare the different treatments – no asterisk – ns, * - $P < 0.05$.

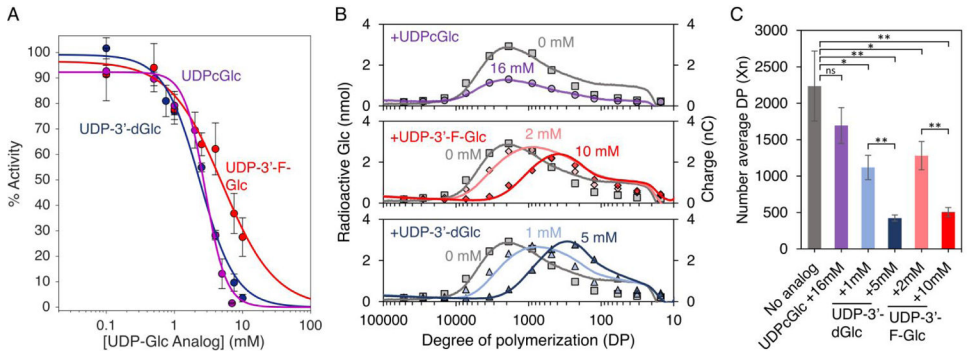


**Figure 9.**

Effects of the blocked substrate analogs on the length of (1,3)-β-D-glucan. (*A*) GS activity in the presence of varying concentration of UDPcGlc (circles, purple trace), UDP-3'-dGlc (diamonds, blue trace) and UDP-3'-F-Glc (squares, red trace). Each data point is an average of three repeats, and error bars represent standard deviation. The solid line is a nonlinear curve fit to the 4-parameter logistic regression. (*B*) Representative SEC-PAD-RC chromatograms for (1,3)-β-D-glucan produced in the presence of UDPcGlc, UDP-3'-F-Glc, and UPD-3'-F-Glc at the indicated concentrations. Discrete data points represent the radioactive quantitation of (1,3)-β-D-glucan shown in the amounts of Glc incorporation (nmol, left axis). The solid traces represent the PAD chromatograms (nC, right axis). (*C*) The number averaged DP (Xn) of (1,3)-β-D-glucan in the presence of substrate analogs. Experiments were performed at least in triplicate, and error bars represent SD. *P* values were calculated using t-tests to compare the different treatments. ns, not significant; * $P < 0.05$; ** $P < 0.01$.

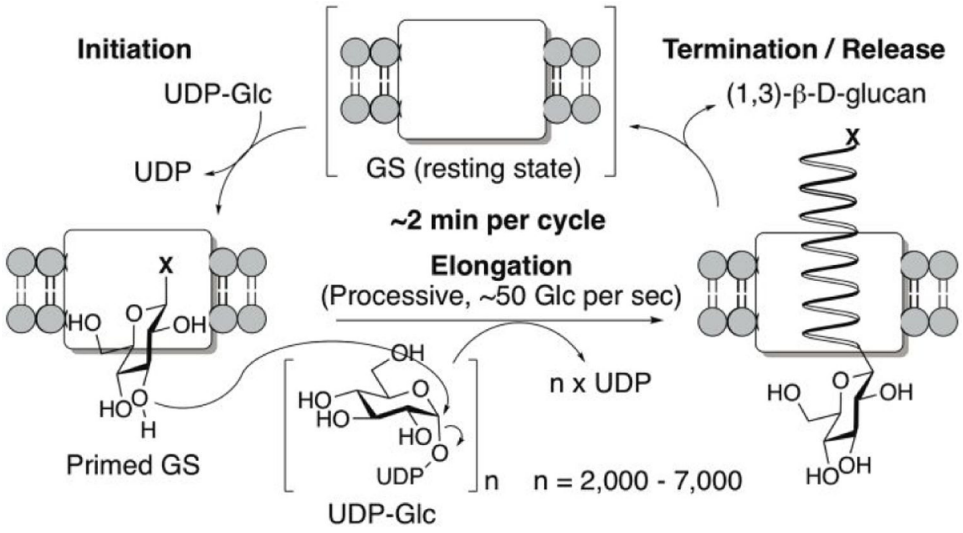


**Figure 10.**

Model of GS catalytic cycle. GS catalyzes self-priming in the absence of exogenously added priming substrate. Subsequent elongation proceeds at the rate of ~50 $sec^{-1}$ until the length reaches 6,550 ± 760 mer, followed by the release of (1,3)-β-D-glucan.

**Table 1.**

Comparison of GS isolated from *S. cerevisiae Δfks2*, *S. cerevisiae Δgas1* and *S. cerevisiae* BY4741.

| Property | ΔFks2-GS | ΔGas1-GS | BY4741-GS |
|---|---|---|---|
| Specific activity (nmol $mg^{-1}$ $min^{-1}$) | 1010 ± 170 | 877 | 685 |
| Elongation (Glc $sec^{-1}$) | 51.5 ± 9.8 | 42.3 ± 5.9 | 46.7 ± 4.3 |
| Glucan at 15s (pmol) | 10.2 ± 3.0 | 9.2 ± 0.9 | 13.0 ± 1.2 |
| Glucan formation[1] ($min^{-1}$) | 0.47 ± 0.11 | 0.50 ± 0.08 | 0.56 ± 0.06 |

[1]Calculated by dividing the rate of elongation by the average Xn of the (1,3)-β-D-glucan obtained between 5–60 min